Inorganic Chemistry

Article

pubs.acs.org/IC

Vanadium Bisimide Bonding Investigated by X-ray Crystallography, ^{51}V and ^{13}C Nuclear Magnetic Resonance Spectroscopy, and V $L_{3,2}$-Edge X-ray Absorption Near-Edge Structure Spectroscopy

Henry S. La Pierre,[†,∥] Stefan G. Minasian,[‡,§] Mark Abubekerov,[†] Stosh A. Kozimor,[‡] David K. Shuh,[§] Tolek Tyliszczak,[§] John Arnold,*[,†] Robert G. Bergman,*[,†] and F. Dean Toste*[,†]

[†]Department of Chemistry, University of California, Berkeley, California 94720-1460, United States

[‡]Inorganic, Isotope and Actinide Chemistry, Los Alamos National Laboratory, Los Alamos, New Mexico 87545, United States

[§]Chemical Sciences Division and Advanced Light Source, Lawrence Berkeley National Laboratory, Berkeley, California 94720, United States

Supporting Information

ABSTRACT: Syntheses of neutral halide and aryl vanadium bisimides are described. Treatment of $VCl_2(NtBu)[NTMS(N^tBu)]$, **2**, with PMe_3, PEt_3, PMe_2Ph, or pyridine gave vanadium bisimides via TMSCl elimination in good yield: $VCl(PMe_3)_2(N^tBu)_2$ **3**, $VCl(PEt_3)_2(N^tBu)_2$ **4**, $VCl(PMe_2Ph)_2(N^tBu)_2$ **5**, and $VCl(Py)_2(N^tBu)_2$ **6**. The halide series (Cl–I) was synthesized by use of TMSBr and TMSI to give $VBr(PMe_3)_2(N^tBu)_2$ **7** and $VI(PMe_3)_2(N^tBu)_2$ **8**. The phenyl derivative was obtained by reaction of **3** with $MgPh_2$ to give $VPh(PMe_3)_2(N^tBu)_2$ **9**. These neutral complexes are compared to the previously reported cationic bisimides $[V(PMe_3)_3(N^tBu)_2][Al(PFTB)_4]$ **10**, $[V(PEt_3)_2(N^tBu)_2][Al(PFTB)_4]$ **11**, and $[V(DMAP)(PEt_3)_2(N^tBu)_2][Al(PFTB)_4]$ **12** (DMAP = dimethylaminopyridine, PFTB = perfluoro-*tert*-butoxide). Characterization of the complexes by X-ray diffraction, ^{13}C NMR, ^{51}V NMR, and V $L_{3,2}$-edge X-ray absorption near-edge structure (XANES) spectroscopy provides a description of the electronic structure in comparison to group 6 bisimides and the bent metallocene analogues. The electronic structure is dominated by π bonding to the imides, and localization of electron density at the nitrogen atoms of the imides is dictated by the cone angle and donating ability of the axial neutral supporting ligands. This phenomenon is clearly seen in the sensitivity of ^{51}V NMR shift, ^{13}C NMR $\Delta\delta_{\alpha\beta}$, and L_3-edge energy to the nature of the supporting phosphine ligand, which defines the parameters for designing cationic group 5 bisimides that would be capable of breaking stronger σ bonds. Conversely, all three methods show little dependence on the variable equatorial halide ligand. Furthermore, this analysis allows for quantification of the electronic differences between vanadium bisimides and the structurally analogous mixed Cp/imide system $CpV(N^tBu)X_2$ ($Cp = C_5H_5^{1-}$).

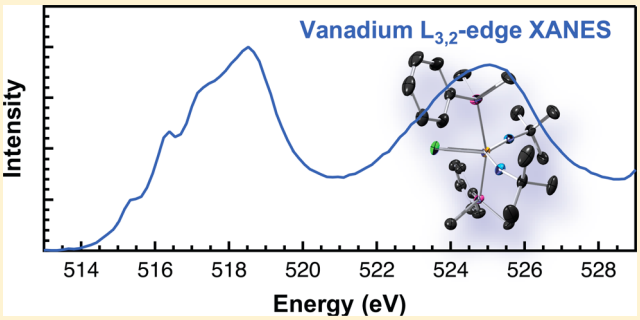

INTRODUCTION

Early metal imido chemistry continues to receive significant attention. Novel forms of stoichiometric and catalytic reactivity continue to be discovered in which imido groups are key supporting groups or intimately involved in the activation of small-molecule substrates.[1−15] Transition metal bisimido complexes in particular have received renewed attention in the past decade.[16−23] Such complexes represent the conceptual union of two of the major driving concepts in organometallic chemistry:[24−30] metallocenes and reactive metal−ligand multiple bonds (because of the structural analogy between 1 σ and 2 π donor ligands). As a result, a large number of bisimido complexes have been isolated and characterized for metals in groups 6−8, and a significant body of coordination and reactivity chemistry has been produced.[25,26,31]

Bisimides are most common in group 6, where Nugent and Wilkinson and co-workers developed their coordination chemistry extensively.[26,32−40] These studies illuminated the fundamentals of bonding in these systems and provided access to model systems for propylene ammoxidation via the [3,3] rearrangement of allylic alcohols to allylic amines.[41,42] Schrock and co-workers[27,43−45] further developed the chemistry of d^2 group 6 and 7 complexes, affording the first examples of bisimido complexes that give access to their metal frontier orbitals, which are isolobal to those in bent metallocenes. These complexes bind small unsaturated molecules such as alkynes, olefins, and organic carbonyls. The d^4 group 8 complexes present similar reactivity.[46] The d^0 group 8 bisimides, developed by Sharpless and co-workers,[47] have led to the development of stoichiometric diamination of alkenes and alkynes. The much more limited chemistry of group 5 bisimide

Received: August 13, 2013
Published: September 11, 2013

   dx.doi.org/10.1021/ic4020543 | *Inorg. Chem.* 2013, 52, 11650−11660

Scheme 1. Synthesis of Neutral and Cationic Vanadium Bisimides[a]

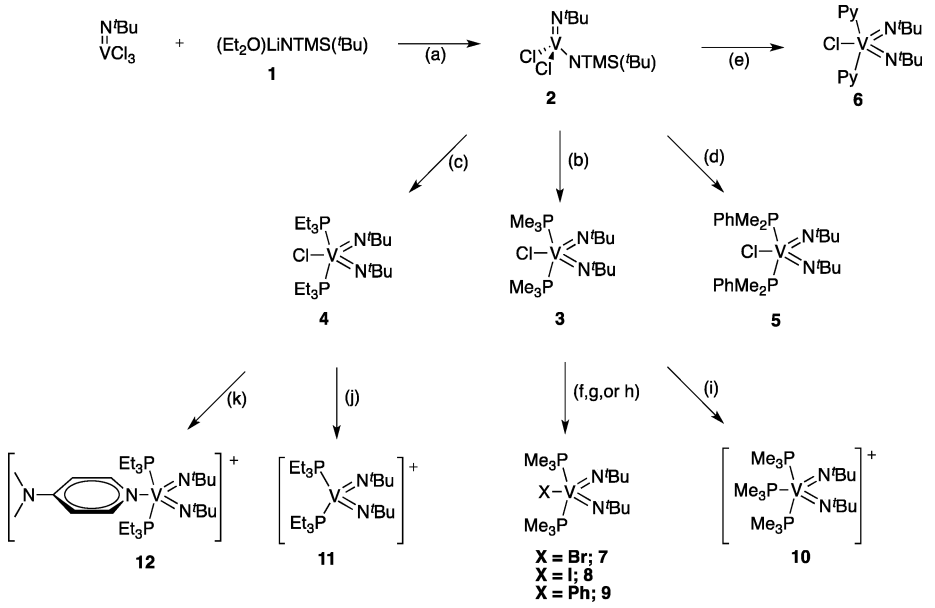

[a]In complexes **10**–**12** the counteranion, $[Al(PFTB)_4]^-$, is not depicted for clarity. Conditions: (a) pentane, −42 °C for 1 h, rt for 6 days, 68%; (b) 2.2 equiv of PMe_3, toluene, reflux, 16 h, 77%; (c) 2.0 equiv of PEt_3, toluene, reflux, overnight, 83%; (d) 2.0 equiv of PMe_2Ph, toluene, reflux, 18 h, 74%; (e) 2.0 equiv of pyridine, toluene, reflux, 16 h, 33%; (f) 1.1 equiv of TMSBr, toluene, reflux, 16 h, 31%; (g) 1.0 equiv of TMSI, toluene, reflux, 16 h, 39%; (h) 1.2 equiv of Ph_2Mg, −72 °C for 1 h, rt for 4 h, 18%; (i) 3 equiv of PMe_3, 1 equiv of $Li[Al(PFTB)_4]$, PhCl, 75%; (j) 1 equiv of $Li[Al(PFTB)_4]$, DCE, 47%; (k) 1 equiv of DMAP, 1 equiv of $Li[Al(PFTB)_4]$, $PhCF_3$, 50%.

chemistry, however, presents two key examples of σ C−H bond addition to transient vanadium or tantalum bisimides supported by the bulky ~Si(^{t}Bu)$_3$ imido capping group.[48,49]

This stoichiometric σ C−H bond activation chemistry drove our reexamination of group 5 bisimido chemistry. The Toste lab[50−53] has recently examined the $ReIO_2(PPh_3)_2$-catalyzed hydrosilylation of ketones and imines. This reaction proceeds via [1,2]-addition of a silane σ Si−H bond across a rhenium oxo. We hypothesized that a properly ligated group 5 bisimide analogue of $ReIO_2(PPh_3)_2$ would allow the activation of less polarized H−H and C−H σ bonds. Such stoichiometric reactivity is well-precedented for group 4 and 5 imido complexes.[48,49,54−62] Furthermore, Nikonov and co-workers[16−18,63,64] have shown that d^2 group 6 bisimides and group 5 Cp/imido complexes are competent catalysts for hydrosilylation. While these systems depend on the d^0/d^2 redox couple to activate silanes, they serve as a significant guidepost for developing catalytic reactivity based on bent metallocene analogues.

The first significant challenge in developing vanadium bisimido complexes for the activation σ bonds is largely synthetic: simply very few group 5 bisimides are known (V,[49,65−70] Nb,[12,71] and Ta[48,71]). Herein we report the synthesis and characterization of neutral and cationic vanadium bis-*tert*-butyl imido complexes supported by monodentate phosphines and pyridine. These studies provide a rare opportunity for the evaluation of bisimido electronic structure by four complementary methods: ^{13}C NMR, ^{51}V NMR, X-ray crystallography, and vanadium $L_{3,2}$-edge X-ray absorption near-edge structure (XANES) spectroscopy. This detailed analysis illuminates the dominant features of the electronic structure of bisimides, which are formal structural analogues of group 6 bisimido, group 5 mixed Cp/imido, and group 4 bent metallocene complexes.

RESULTS AND DISCUSSION

Synthesis of Neutral Chloro Vanadium Bisimides. At the start of our studies, there were just three extant vanadium bisimido species, and subsequently three more examples appeared in the literature. These complexes are either supported as their anionic -ate complexes[68] or employ bulky supporting ligands to enforce kinetic stability.[49,65−67,69,70] Although these syntheses defined reliable routes to vanadium bisimides, they did not provide modular access to sterically unencumbered complexes. The known complexes also were not supported by labile ligands and, as a result, do not afford access to the reactive bisimido moiety.[22] Therefore, they were not amenable to the development of catalytic reactions analogous to the reactivity observed for $ReIO_2(PPh_3)_2$. Three general approaches for the synthesis of vanadium bisimides were considered: (1) reduction of organic azides by a d^2 imide; (2) base-induced α-NH elimination of a mixed alkyl, primary amide, vanadium imide; and (3) base-induced α-NTMS elimination of a mixed halo, silyl amide, vanadium imide.

The first approach was not pursued as it required employing bulky supporting ligands for the low-valent imide and would not have provided a modular synthesis. The second approach required the synthesis of trialkyl vanadium imides. In the case of aryl imides, these complexes are well-known and readily produced. However, in the case of *tert*-butyl vanadium imides, there is little literature precedent for trialkyl complexes of this type, and in our hands, treatment of V(N^{t}Bu)Cl$_3$ with common alkylating agents such as KCH_2Ph, $LiCH_2TMS$ (TMS = trimethylsilyl), and $LiCH_2C(CH_3)_3$ yielded only intractable mixtures, presumably due to complications from reduction of V(V) to V(IV), as has been noted by other researchers.[68] The third approach, however, appeared most promising. The use of a Lewis base-induced elimination of TMSCl was inspired by the methodology for generating Cp*TiCl$_3$ from $TiCl_4$ and

dx.doi.org/10.1021/ic4020543 | Inorg. Chem. 2013, 52, 11650−11660

Cp*TMS (Cp* = C_5Me_5), a method that avoids inadvertent reduction of $TiCl_4$ to $TiCl_3$ by Cp*M (M = alkali metal). Thus, treating Preuss's $V(N^tBu)Cl_3$[72] with Et_2O·LiNTMS(^{t}Bu), **1**, gave $VCl_2(NtBu)(NTMS(^tBu)$, **2**, in 68% yield as red/orange crystals (Scheme 1). This reaction is very sensitive to reaction conditions and stoichiometry. Any excess Et_2O·LiNTMS(^{t}Bu) or the use of LiNTMS(^{t}Bu) gives the deep blue vanadium(IV) dimer $[V(NTMS(^tBu))Cl)_2(\mu\text{-}NtBu)_2]$, which was originally described by Preuss et al.[68] In order to achieve best results, it is advisable to recrystallize Et_2O·LiNTMS(^{t}Bu) from Et_2O twice to ensure a 1:1 ratio of Et_2O to lithium amide.[73] In the event that the reduced side product is formed, it can be separated via fractional crystallization from pentane at −80 °C. At room temperature in C_6D_6, $VCl_2(N^tBu)[NTMS(^tBu)]$ is a mixture of two isomers resulting from isomerization about the V−N amide bond, both of which are extremely soluble in hydrocarbons. This latter property has hindered its crystallographic characterization as it readily dissolves in the Paratone-N oil employed to mount crystals. While $VCl_2(N^tBu)[NTMS(^tBu)]$ is best purified by crystallization, it can be distilled at 120 °C at ∼0.1 mmHg without decomposition or loss of TMSCl.

In contrast to this observed thermal stability, the addition of 2.0−2.2 equiv of small Lewis bases induces the elimination of TMSCl in refluxing toluene. Pyridine, PMe_3, PEt_3, or PMe_2Ph all produce stable five-coordinate distorted trigonal bipyramidal complexes in low to good yield (33−84%) after crystallization (Scheme 1). The geometric parameters for complexes **5** and **6** are presented in Table 1, and the details of their spectroscopic characterization are presented in the following discussion. Structural data and synthetic procedures for **3** and **4** have been published.[21,22] This Lewis base-induced TMSCl elimination from **2** is not general; no reaction occurs with phosphines with cone angles larger than that of PEt_3 (132°): Ph_2Me, P^tBu_2Ph, PPh_3, P^iPr_3, and PCy_3.

Table 1. Selected Bond Lengths and Angles of Complexes 5, 6, 8, and 9

	5	6[a]	8[b]	9
		Bond Lengths (Å)		
N_{im}−V	1.696(2); 1.685(2)	1.6852(17); 1.6873(17)	1.669(5); 1.684(4); 1.687(5)	1.707(5); 1.718(5)
L−V[c]	2.4756(7); 2.4646(8)	2.1626(17); 2.1662(17)	2.4548(16); 2.4703(16); 2.4545(11)	2.4264(18); 2.4375(19)
X−V[d]	2.4175(7)	2.4329(7)	2.8370(11); 2.8201(12)	2.175(5)
		Bond Angles (deg)		
C−N_{im}−V	161.2(2); 173.21(19)	167.73(15); 161.83(15)	168.5(5); 168.1(3); 166.5(4)	172.0(4); 160.6(4)
N_{im}−V−N_{im}	116.14(10)	113.83(8)	116.4(2)	119.6(2)
N_{im}−V−X[c]	123.21(7); 120.65(8)	127.55(6); 118.57(6)	118.58(18); 124.97(18)	116.4(2); 124.0(2)
X−V−L[c,d]	78.79(3); 82.67(2)	82.14(5); 81.05(5)	81.73(4); 83.77(5); 84.00(5)	79.39(15); 79.09(15)
L−V−L[d]	160.67(3)	162.60(6)	167.77(7)	158.26(6)

[a]Data for one of two molecules in an asymmetric unit are provided. [b]Mirror plane bisects two molecules in asymmetric unit; therefore, there are 2−3 independently refined values. [c]L = Py N-atom or phosphine P-atom. [d]X = Cl, Br, I, or phenyl *ipso*-C.

Derivatization of Neutral Vanadium Bisimides. The parent bis-PMe_3 complex **3** is readily transformed into its heavier halide congeners. Treatment of **3** in toluene with 1 equivalent of either TMSBr or TMSI gives the corresponding bromide or iodide complexes **7** and **8** in reasonable yields (31% and 39%) (Scheme 1). As described in detail below, this halide series possesses very similar ^{51}V NMR shifts. As such, clean conversion of the equatorial halides was confirmed by elemental and crystallographic analysis. The ORTEP representation of **8** is shown in Figure 1 (bond lengths and angles are presented in Table 1), and like its chloride precursor, it has a distorted trigonal bipyramidal structure with τ = 0.77 (τ = 1.00 for an ideal trigonal bipyramid and 0.00 for an ideal square pyramid). Although the bromide **7** crystallizes readily from hexane, single-crystal X-ray diffraction was of limited utility due to whole-molecule disorder in the solid state. Attempts to complete the halo series with synthesis of the fluoride derivative were unsuccesful: trimethyltin fluoride did not undergo exchange with the chloride in refluxing toluene.

Reactions of **3** with common alkylating reagents were pursued in order to access simple organometallic derivatives. As with other high-valent vanadium systems, these reactions gave intractable mixtures, presumably due to the reduction of V(V) to V(IV).[68,74] While 1 equiv of KCH_2Ph, $LiCH_2TMS$ (TMS = trimethylsilyl), $LiCH_2C(CH_3)_3$, and MeLi failed to give the monoalkyl derivatives, the dialkylmagnesium reagent Me_2Mg did not react, which is surprising given that similar reagents have been shown to give d^0 vanadium alkyls without significant reduction. All attempts to synthesize a vanadium hydride by use of ionic reagents ($NaBH_4$ or aluminum hydride reagents such as $LiAlH_4$ or Red-Al) gave similar intractable mixtures, and no reaction was observed with triethylsilane.[75] While the reactivity of **3** with aryl lithium and Grignard reagents was similar to that of their alkyl equivalents, **3** underwent salt metathesis with 1 equivalent of Ph_2Mg to give $VPh(PMe_3)_2(N^tBu)_2$ **9** in low yield (18%, Scheme 1). The complex crystallizes from hexane as yellow plates. The ORTEP diagram of **9** is presented in Figure 1. Like the halide derivatives, **9** is also a distorted trigonal bipyramid with τ = 0.56. Crystallographically characterized d^0 vanadium, σ-bonded phenyl complexes are rare; nonetheless, metrical parameters of **9** match well with the only previously reported complex.[76]

X-ray Crystallography. Solid-state structures for complexes **3**−**6**, **8**−**10**, and **12** have been determined by X-ray crystallographic studies. All compounds are distorted trigonal bipyramids with τ between 0.50 and 0.77. For the chloride series $VCl(N^tBu)_2(L)_2$, where L = PMe_3, PEt_3, PMe_2Ph, and Py, the V−Cl bond lengths are essentially invariant (between 2.43 Å for **6** and 2.41 Å for **5**). Likewise, the V−N_{im} bond lengths change little from approximately 1.68 ± 0.03 Å. However, there are subtle changes in the V−P bond lengths, and P−V−P (or N_{py}), N_{im}−V−N_{im}, and V−N_{im}−C bond angles. In the three phosphine-supported complexes **3**−**5**, the V−P bond lengths scale with the cone angle (Θ) for the corresponding phosphine: Θ for PMe_3 = 118°,[77] for PMe_2Ph = 122°,[78] and for PEt_3 = 132°.[77] That is, the shortest V−P bond lengths are observed for the PMe_3 complex **3** at 2.4507(7) and 2.4546(7) Å; **5** follows with 2.4756(7) and 2.4646(8) Å; and finally **4** with 2.4999(14) and 2.5006(14) Å.

While the P−V−P angles for the complexes also increase with larger cone phosphine cone angles [**3**, 160.93(2)°; **5**, 160.67(3)°; **4**, 161.14(5)°], the N_{im}−V−N_{im} angles follow the inverse trend and decrease with bulkier phosphines [**4**, 114.0(2)°; **5**, 116.14(10)°; **3**, 115.88(10)°]. All of these N_{im}−V−N_{im} angles lie below the ideal angle of 120°, a feature

dx.doi.org/10.1021/ic4020543 | Inorg. Chem. 2013, 52, 11650−11660

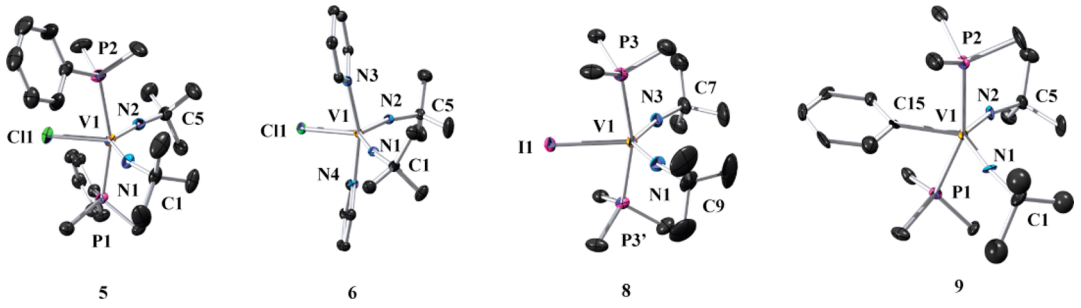

Figure 1. Molecular structures of complexes **5**, **6**, **8**, and **9**. Thermal ellipsoids are drawn at 50% probability level. Hydrogen atoms have been removed for clarity.

that is common to group 5 bisimides,[48] regardless of the nature of the imido R group. This feature has been rationalized on the basis of an electronic argument, whereby the imido ligands are better σ and π donors relative to the axial supporting ligands. Therefore, the contraction of the $N_{im}-V-N_{im}$ angle serves to increase effective overlap with the metal atomic orbitals.[48] As such, the contraction of this angle with increasing cone angle of the supporting phosphine implies that the contraction is the result of less effective donation of electron density to the metal center by the more sterically hindered phosphine. There is no apparent trend in the $V-N_{im}-C$ bond angles for the four chloride complexes. On average these angles are 168°. However, they cover the range of 160°−171°, and none of the complexes have equivalent $V-N_{im}-C$ angles. This phenomenon is likely caused by crystal packing forces rather the intrinsic electronic properties of the complexes.

The substitution of phenyl or iodide ligands for chloride in **3** results in changes in the key parameters of the bisimido complexes. In complex **9**, the phenyl ring is coplanar with the equatorial plane of the trigonal bipyramid. This results in a slight diminishing of the P−V−P angle to 158.26(6)°, contraction of the V−P bonds to 2.4264(18) and 2.4375(19) Å, and expansion of the $N_{im}-V-N_{im}$ angle to 119.6(2)°. These changes combine to give $\tau = 0.56$. In the iodide complex **8**, the larger iodide substituent leads to expansion of the P−V−P angle to 167.77(7)°, despite the longer V−halogen bond compared to **3**. However, the V−P bonds lengths are nearly identical to those of the chloride at 2.4548(16) and 2.4703(16) Å [2.4545(11)]. As a result, the $N_{im}-V-N_{im}$ angle widens to 116.4(2)°.

^{13}C NMR Spectroscopy. The change in ^{13}C NMR chemical shift ($\Delta\delta_{\alpha\beta}$) of the tertiary carbon (C_α) and methyl carbons (C_β) of the *tert*-butyl imido group can provide a qualitative indication of the degree of charge localization at the imido nitrogen and, hence, the nucleophilicity of the imide.[79] A decrease in electron density at nitrogen leads to a downfield shift in C_α and an upfield shift in C_β. Therefore, an increase in the difference in the shifts of the resonances indicates a decrease in the localization of electron density at nitrogen.

Other studies have correlated trends in $\Delta\delta_{\alpha\beta}$ with other changes in the electronegativity of the metal or the ligand set.[8] For the vanadium bisimides discussed here, an increase in $\Delta\delta_{\alpha\beta}$ would be predicted if there is an increase in the electronegativity of the metal or complete ligand set. In contrast, data for the series of halide complexes **3**, **7**, and **8** (Table 2) shows that $\Delta\delta_{\alpha\beta}$ decreases with increasing electronegativity of the equatorially bound halide. In other words, the chloride complex has the lowest $\Delta\delta_{\alpha\beta}$ and the greatest localization of charge density at nitrogen. This effect implies that chloride more effectively donates electron density in an inductive fashion to the nitrogen atoms via the central vanadium. The basis of this trend is likely the more effective overlap of the compact chloride 3p orbitals with the vanadium 3d-based fragment orbitals than that of the more diffuse bromide 4p or iodide 5p orbitals.

Table 2. Comparison of $\Delta\delta_{\alpha\beta}$ Values for Complexes 3−12

compd	$\Delta\delta_{\alpha\beta}$, ppm
$V(Cl)(PMe_3)_2(N^tBu)_2$, **3**	34.4
$V(Cl)(PEt_3)_2(N^tBu)_2$, **4**	34.4
$V(Cl)(PMe_2Ph)_2(N^tBu)_2$, **5**	36.2
$V(Cl)(Py)_2(N^tBu)_2$, **6**	27.1
$V(Br)(PMe_3)_2(N^tBu)_2$, **7**	35.4
$V(I)(PMe_3)_3(N^tBu)_2$, **8**	36.4
$V(Ph)(PMe_3)_2(N^tBu)_2$, **9**	*a*
$[V(PMe_3)_2(N^tBu)_2]^{1+}$, **10**	*a*
$[V(PEt_3)_2(N^tBu)_2]^{1+}$, **11**	29.8
$[V(DMAP)(PEt_3)_2(N^tBu)_2]^{1+}$, **12**	39.9

*a*The α-*t*Bu resonance was not located.

For the chloride series supported by different phosphines, $\Delta\delta_{\alpha\beta}$ is sensitive to the electron-donating ability of the corresponding phosphine. Both the PMe_3 complex **3** and the PEt_3 complex **4** have identical $\Delta\delta_{\alpha\beta}$ values (34.4 ppm) as both are electron-rich trialkylphosphines. The PMe_2Ph complex **5** has a larger $\Delta\delta_{\alpha\beta}$ (36.2 ppm), presumably because the imide ligands compensate for the less electron-donating PMe_2Ph ligands by donating more electron density to the electropositive metal center. A similar trend was observed for two of the cationic complexes, **11** and **12**. The four-coordinate complex **11** has a $\Delta\delta_{\alpha\beta}$ of 39.9 ppm, reflecting the extremely electron-poor metal center. Upon the coordination of DMAP to form complex **12**, $\Delta\delta_{\alpha\beta}$ shifts to 29.8 ppm, which indicates that there is more strongly localized electron density in the cationic complexes in comparison to the neutral five-coordinate complexes.

^{51}V NMR Spectroscopy. The reported shift range for $\delta(^{51}V)$ spans 5000 ppm, reflecting the sensitivity of the vanadium nucleus to its electronic environment.[80] Unlike ^{1}H or ^{7}Li NMR, ^{51}V NMR shifts do not necessarily correlate directly with electronic shielding of the nucleus and thus do not correlate with oxidation state.[80] However, within an isostructural series, shielding trends can be defined that can be used to infer changes in ligand field. Previously, it has been empirically observed that high-valent (d^0), open-shell systems such as VOX_3, $VN(p\text{-tol})X_3$, and $CpVN^tBuX_2$ follow an "inverse electronegativity dependence" on the nature of X^{1-} σ-bonded supporting ligands; that is, less electronegative and more

dx.doi.org/10.1021/ic4020543 | *Inorg. Chem.* 2013, 52, 11650−11660

polarizable ligands lead to deshielding.[80] The case of $CpVN^tBuX_2$ is particularly interesting in that it is the mixed Cp/imido isolobal analogue of the complexes presented here. The ^{51}V NMR shifts of $CpVN^tBuX_2$ complexes (for X = Cl, Br, I, and Me) are shown in Table 3, along with the ^{51}V NMR shifts of the complexes from this study. Clearly the trend for $CpVN^tBuX_2$ complexes does not hold for $VX(PMe_3)_2(N^tBu)_2$. In fact no trend was identified for the halo/aryl series, and by examining the reported shifts for the different phosphine-supported vanadium chloride complexes (**3**, **4**, and **5**), therefore the ^{51}V NMR shift is solely dependent on the nature of the phosphorus supporting ligand in this isostructural series.

Table 3. Comparison of ^{51}V NMR Values for Complexes 3−12

compd	δ, ppm
$V(Cl)(PMe_3)_2(N^tBu)_2$, **3**	−782.31
$V(Cl)(PEt_3)_2(N^tBu)_2$, **4**	−757.33
$V(Cl)(PMe_2Ph)_2(N^tBu)_2$, **5**	−766.92
$V(Cl)(Py)_2(N^tBu)_2$, **6**	−485.42
$V(Br)(PMe_3)_2(N^tBu)_2$, **7**	−770.95
$V(I)(PMe_3)_2(N^tBu)_2$, **8**	−778.38
$V(Ph)(PMe_3)_2(N^tBu)_2$, **9**	−801.07
$[V(PMe_3)_3(N^tBu)_2]^{1+}$, **10**	−792.29
$[V(PEt_3)_2(N^tBu)_2]^{1+}$, **11**	−278.99
$[V(DMAP)(PEt_3)_2(N^tBu)_2]^{1+}$, **12**	−728.16
$CpV(N^tBu)Cl_2$[a]	−457
$CpV(N^tBu)Br_2$[a]	−329
$CpV(N^tBu)I_2$[a]	−110
$CpV(N^tBu)Me_2$[a]	−25

[a]From refs 116−118.

These phenomena can be explained by considering contributions for overall shielding.[80] It is composed of three parts: the local diamagnetic term, the local paramagnetic term, and the nonlocal term. Of these, the second is by far the most important. Most pertinent to the question at hand are results of Maatta and co-workers,[74] which demonstrate that, for the related system $VN(p\text{-tol})X_3$, two types of electronic transitions contribute to local paramagnetic term: $\pi \rightarrow \pi^*$ and $\sigma \rightarrow \pi^*$. For a given isostructural imide or bisimide system the $\pi \rightarrow \pi^*$ transition changes little, but changing X changes the energy of the $\sigma \rightarrow \pi^*$ transition and hence the magnitude of the local paramagnetic term. If it is assumed that this model holds for the similar bisimide system presented here, the independence of chemical shift on the electronegativity of the supporting ligand can be explained. In the case of $VX(PMe_3)_2(N^tBu)_2$ complexes, the V−X σ bond is orthogonal to the π^* system of the bisimide ligands and there is little overlap. Therefore, there is no defined electronegativity trend observed in the ^{51}V NMR spectra of the halide series **3**, **7**, and **8**. In the case of the trend observed for the supporting phosphine complexes **3**−**5**, the deshielding local paramagnetic term increases with increasing cone angle and relative electron donation of the phosphine ligand and the corresponding V−P bond length. In other words, the overall shielding in the ^{51}V NMR spectra is governed by the $\sigma \rightarrow \pi^*$ transition from the V−P σ bonds to the π^* orbitals of the bisimide moiety. This dependence of ^{51}V NMR resonance on the nature of the supporting phosphine ligand indicates that the charge distribution within the bisimido moiety and, hence, reactivity can controlled by judicious choice of supporting ligand. This conclusion is also supported by analysis of the vanadium $L_{3,2}$-edge XANES.

Vanadium $L_{3,2}$-Edge XANES. Bent metallocenes have been the subject of numerous investigations by X-ray absorption spectroscopies,[81−86] but relatively little has been reported with bisimido compounds.[87] Vanadium L_1- and $L_{3,2}$-edge XANES has been used to characterize a variety of vanadium oxides,[88−98] particularly V_2O_5.[99−107] However, few applications of V L-edge spectroscopy have been reported for molecular systems,[108,109] and to the best of our knowledge, none contain high-valent vanadium supported by imide ligands.

In this study, vanadium $L_{3,2}$-edge XANES were obtained in transmission mode by use of a scanning transmission X-ray microscope (STXM) for samples of **3**−**11** to corroborate the geometric and electronic trends described above (Figure 2). For each d^0 V complex, the $L_{3,2}$-edge absorptions arise from dipole-allowed $2p^6\ 3d^0 \rightarrow 2p^5\ 3d^1$ transitions, which are split by roughly 7 eV into two primary L_3 ($2p_{3/2}$) and L_2 ($2p_{1/2}$) edges due to spin−orbit coupling of the core hole.[110,111] Each of the L_3 and L_2 edges are subject to additional splitting due to ligand field and multiplet effects, though fine structure on the L_2 edge is typically not resolved due to broadening from Coster−Kronig Auger decay processes.[112,113] The position and splitting of the sharp transitions comprising the L_3-edge can be sensitive to differences in oxidation state, ligand field, and local geometry.[114]

The presence or absence of individual features in the L_3-edges was determined by inspection of a plot of the second derivative of the absorption, as described previously (Figure 2 and Table 4).[82,83,115] The L_3-edge XANES spectra for **3**−**11** each contain well-resolved shoulders and additional peaks for **5** and **7**, on the low-energy side of the L_3-edge maximum. Relative differences in the ligand field splitting dictated by the two imide ligands can be evaluated by comparing the relative intensities of the final state multiplets.

Upon examination of the spectral profiles observed for **3**−**11**, it is apparent that each spectrum contains a similar well-resolved transition with an average position of 517.3 ± 0.1 eV. For **3**, **4**, **8**, **10**, and **11** this transition constitutes the absorption maximum for the L_3-edges. However, for both **5** and **7**, the absorption maximum is 1.3 eV higher in energy (518.6 eV). Related high-energy transitions are observed in the spectra of **3**, **4**, **8**, **10**, and **11**, but they are represented as a shoulder near 518.2 ± 0.2 eV along the high-energy side of the absorption maximum. The change in spectral profile and accompanying increase in the position of the absorption maximum is suggestive of a different bonding mode in **5** and **7** relative to **3**, **4**, **8**, **10**, and **11**.

To understand the origin of these changes, it is instructive to compare the $L_{3,2}$-edge XANES spectra with data from the ^{13}C and ^{51}V NMR studies discussed above. First, the energy of the L_3-edge absorption maximum does not change systematically with the halide electronegativities in the $VX(PMe_3)_3(N^tBu)_2$ compounds (V = Cl, Br, I) when the halide changes from chloride (517.2 eV for **3**) to bromide (518.6 eV for **7**) to iodide (517.2 eV for **8**). A similar phenomenon was observed in the trend of ^{51}V NMR chemical shifts for **3** (−782.31 ppm), **7** (−770.95 ppm), and **8** (−778.38 eV). In addition, the L_3-edge absorption maximum does not change significantly upon abstraction of a Cl^{1-} ligand from **4** (517.4 eV) to form the four-coordinate cation **11** (517.2 eV). Taken together, the results suggest that bonding with the equatorial bromide ligand is enhanced in **7** but that the V−I interaction is more ionic,

dx.doi.org/10.1021/ic4020543 | Inorg. Chem. 2013, 52, 11650−11660

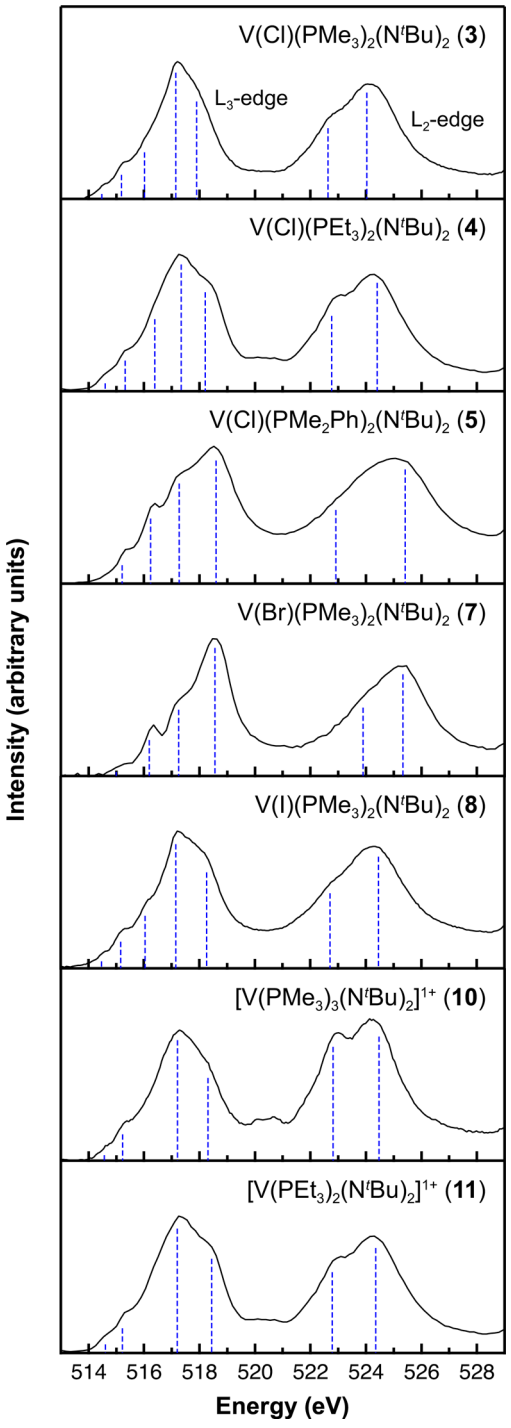

Figure 2. Vanadium $L_{3,2}$-edge XANES spectra of compounds **3**–**5**, **7**, **8**, **10**, and **11**. Peak and shoulder positions are determined from the second derivative of the spectrum and indicated with vertical dashed blue lines.

such that the ^{51}V NMR spectra and L_3-edge XANES are similar to those found for the cations and the chloride complexes.

Next, the L_3-edge increases in energy in the series of $VCl(PR_3)_2(N^tBu)_2$ when the alkyl substituents on the phosphine change from PMe_3 (517.2 eV for **3**) to PEt_3 (517.4 eV for **4**) to PMe_2Ph (518.6 eV for **5**). While the PMe_3 and PEt_3 ligands in **3** and **4** have similar electron-donating/withdrawing properties, the PMe_2Ph ligands in **5** are more electron-withdrawing than either trialkyl-substituted phosphine. This trend correlates with the values of $\Delta\delta_{\alpha\beta}$ from ^{13}C NMR for **3** (34.4 ppm), **4** (34.4 ppm), and **5** (36.2 ppm). As discussed above, the PMe_2Ph substitution in **5** induces greater donation from the imide ligands and enhances V–N σ bonding. This interaction further destabilizes the 3d orbitals on V and raises the energy of the L_3-edge transitions observed for **5** relative to **3** and **4**. In addition, incorporation of a more electron-withdrawing phosphine appears to turn on low-energy transitions at 516.3 and 517.3 eV, which may be a consequence of enhanced V–P π bonding in **5**. Additional structural, spectroscopic, and theoretical measurements are currently underway to validate these interpretations. However, these comparisons suggest that subtle differences in the electronic properties of the supporting phosphine ligands can lead to a significant difference in the electronic structure reflected by V $L_{3,2}$-edge XANES, which may have important consequences for tuning electronic structure and reactivity in catalysis.

CONCLUSION

The synthesis of a series of isostructural vanadium bisimido complexes was accomplished, a key step being the Lewis base-induced elimination of TMSCl to form the bisimido core. These compounds served as a base for the synthesis of a variety of neutral halo and aryl complexes and cationic complexes. These synthetic methods provided access to a unique system to evaluate electronic structure by a variety of methods. ^{13}C NMR revealed qualitatively that the degree of electron localization at the imido nitrogens decreases on the formation of four-coordinate cations but increases on the formation of five-coordinate cations and is largely dependent on the cone angle and donating ability of the axial neutral supporting ligands. Vanadium $L_{3,2}$-edge X-ray absorption spectra from scanning transmission X-ray microscopy measurements confirm the presence of V^{5+} and closely resemble trends observed from ^{51}V NMR. Taken together, both techniques are sensitive enough to discriminate between subtle differences in the steric environments imposed by the neutral supporting ligands as confirmed by the crystallographic studies. However, such subtle changes between all five-coordinate complexes, both neutral and cationic, suggests that local electron density at vanadium is mostly dominated by the covalent multiple-bond interactions with the imide ligands. This result stands in contrast to the shielding trends observed for the well-studied mixed imido Cp system $CpVNRX_2$ (where X = Cl, Br, I, and Me).[116−118]

In summary, the localization of electron density at imide nitrogen is dictated by the cone angle and donating ability of the axial neutral supporting ligands (phosphine or pyridine), not the nature of the variable equatorial ligand (Cl^-, Br^-, I^-, or Ph^-). This phenomenon is clearly seen in the insensitivity of ^{51}V NMR shift, ^{13}C NMR $\Delta\delta_{\alpha\beta}$, and L_3-edge energy to the nature of the equatorial substituent. Nonetheless, all three methods show a clear dependence on the supporting ligands, which suggests that the larger cone angle electron-rich phosphines—especially those that would support four-coordinate cationic complexes—might be sufficient to cleave stronger σ C–H bonds (relative to the cleavage of σ H–H bonds of bonds in H_2 as observed for complex **10**).[21]

EXPERIMENTAL SECTION

General Considerations. Unless otherwise noted, all reactions were performed by use of standard Schlenk line techniques or in an MBraun inert atmosphere box under an atmosphere of argon or

dx.doi.org/10.1021/ic4020543 | Inorg. Chem. 2013, 52, 11650−11660

Table 4. Summary of Data Taken from Vanadium L-Edge XANES Spectra Measured in This Study[a]

compd	L_3-edge features, eV	L_2-edge features, eV	$L_2 - L_3$, eV
$V(Cl)(PMe_3)_2(N^tBu)_2$, **3**	514.5(sh), 515.2 (sh), 516.0 (sh), 517.2* (p) 517.9 (sh)	522.6 (sh), 524.1* (p)	6.9
$V(Cl)(PEt_3)_2(N^tBu)_2$, **4**	514.6 (sh), 515.3 (sh), 516.4 (sh), 517.4* (p), 518.2 (sh)	522.8 (sh), 524.4* (p)	7.0
$V(Cl)(PMe_2Ph)_2(N^tBu)_2$, **5**	515.2 (sh), 516.3 (p), 517.3 (sh), 518.6* (p)	522.9 (sh), 525.4* (p)	6.8
$V(Br)(PMe_3)_2(N^tBu)_2$, **7**	515.0 (sh), 516.2 (p), 517.3 (sh), 518.6* (p)	523.9 (sh), 525.4* (p)	6.8
$V(I)(PMe_3)_2(N^tBu)_2$, **8**	514.5 (sh), 515.2 (sh), 516.1 (sh), 517.2* (p), 518.3 (sh)	522.7 (sh), 524.5* (p)	7.3
$[V(PMe_3)_3(N^tBu)_2]^{1+}$, **10**	514.6 (sh), 515.2 (sh), 517.3* (p), 518.3 (sh)	522.8 (p), 524.5* (p)	7.2
$[V(PEt_3)_2(N^tBu)_2]^{1+}$, **11**	514.6 (sh), 515.2 (sh), 517.2* (p), 518.5 (sh)	522.8 (p), 524.4* (p)	7.2
V_2O_5	514.8 (p), 515.6 (p), 516.7 (p), 517.8 (p), 518.4* (p), 519.5 (sh)	525.3* (p)	6.9

[a]The absorption maxima on L_3- and L_2-edges are indicated with asterisks. Peak maxima are ±0.08 eV.

dinitrogen (<1 ppm O_2/H_2O), respectively. All glassware and cannulae were stored in an oven at ca. 425 K. Pentane, diethyl ether, toluene, tetrahydrofuran, dichloromethane, and dimethoxyethane were purified by passage through a column of activated alumina and degassed prior to use. C_6D_6 was vacuum-transferred from sodium/benzophenone and degassed with three freeze−pump−thaw cycles. 1,2-$C_2D_4Cl_2$ was vacuum-transferred from CaH_2 and degassed with three freeze−pump−thaw cycles. NMR spectra were recorded on Bruker AV-300, AVB-400, AVQ-400, AV-500, and AV-600 spectrometers. ^1H and $^{13}C\{^1H\}$ chemical shifts are given relative to residual solvent peaks. ^{31}P, ^{51}V, ^{19}F, and ^{27}Al chemical shifts were referenced to external standards [$P(OMe)_3$ at 1.67 ppm, $VOCl_3$ at 0.00 ppm, $CFCl_3$ at 0.00 ppm, and 1 M $Al(NO_3)_3$ in H_2O/D_2O at 0 ppm, respectively]. Proton and carbon NMR assignments were routinely confirmed by $^1H-^1H$ (correlation spectroscopy, COSY) or $^1H-^{13}C$ (heteronuclear single quantum coherence, HSQC, and heteronuclear multiple bond correlation, HMBC) experiments as necessary. Resonances marked with a * were located by HMBC. Infrared (IR) samples were prepared as Nujol mulls and were taken between KBr disks. The following chemicals were purified prior to use: chlorobenzene and $tBuNH_2$ were distilled from CaH_2 and were degassed by bubbling argon through the liquids for 15 min; α,α′,α″-trifluorotoluene ($PhCF_3$), was distilled from P_2O_5 and degassed by bubbling argon through the liquid for 15 min; $LiAlH_4$ was dissolved in Et_2O, filtered, and reduced in vacuo and the residue was heated at 80 °C under vacuum for 2 h; perfluoro-*tert*-butyl alcohol was stored over 4 Å sieves and degassed by three freeze−pump−thaw cycles. PMe_3,[119] $Li[Al(PFTB)_4]$,[120] Ph_2Mg,[121] $VCl_3(N^tBu)$,[122] $Et_2O{\cdot}LiNTMS(^tBu)$, $VCl_2(NtBu)[NTMS(^tBu)]$,[21] $VCl(PMe_3)_2(N^tBu)_2$,[21] $VCl(PEt_3)_2(N^tBu)_2$,[21,22] $[V(PMe_3)_3(N^tBu)_2][Al(PFTB)_4]$,[21] $[V(PEt_3)_2(N^tBu)_2][Al(PFTB)_4]$,[22] and $[V(PEt)_2(N^tBu)_2(DMAP)][Al(PFTB)_4]$[22] were prepared by standard literature procedures. All other reagents were acquired from commercial sources and used as received. Elemental analyses were determined at the College of Chemistry, University of California, Berkeley. The X-ray structural determinations were performed at CHEXRAY, University of California, Berkeley, on Bruker SMART, SMART APEX, APEX II Quazar, or MicroSTAR-H X8 APEXII diffractometers.

Preparation of $VCl(PMe_2Ph)_2(N^tBu)_2$ (5). To a solution of $VCl_2(NtBu)[NTMS(^tBu)]$ (1.56 g, 4.6 mmol) in 50 mL of toluene was added PMe_2Ph (2.0 equiv, 1.32 mL, 4.6 mmol) via syringe. The reaction mixture was brought to reflux for 18 h. It was cooled and reduced to a residue in vacuo and extracted with warm hexane. The solution was transferred to a Schlenk tube via a filter cannula, the filtrate was reduced until the product began crystallize, and the solution was placed into a −40 °C freezer overnight. The title compound was obtained in 74% (1.73 g) yield as light green blocks after decantation. X-ray-quality crystals were grown from a hot hexane solution, which was cooled to room temperature and then stored at −40 °C overnight. ^1H NMR (C_6D_6, 600.1 MHz, 298 K) δ 8.01 (br s, *Ar*, 4H), 7.14 [m (overlapping with residual C_6D_5H), *Ar*, 4H], 7.08 (m, *Ar*, 2H), 1.66 (br s, PMe_2Ph, 12H), 1.31 (s, *tBu*, 18H). $^{13}C\{^1H\}$ NMR (C_6D_6, 150.9 MHz, 298 K) δ 137.09 (br s, *Ar*), 133.24 (s, *Ar*), 129.33 (s, *Ar*), 69.5* (br s, α-*t*Bu), 33.32 (br s, β-*t*Bu) 16.28 (unresolved t, PMe_3). $^{31}P\{^1H\}$ NMR (C_6D_6, 242.9 MHz, 298 K) δ 5.55 (br s, $\Delta\nu_{1/2}$ = 1844.93 Hz). $^{51}V\{^1H\}$ NMR (C_6D_6, 157.7 MHz, 298 K) δ −766.92 (br s, $\Delta\nu_{1/2}$ = 550.33 Hz). Anal. Calcd for $C_{24}H_{40}N_2P_2VCl$: C, 57.09; H, 7.98; N, 5.55. Found: C, 56.92; H, 7.72; N, 5.53. IR (KBr, Nujol, cm^{-1}) 1455 (w), 1435 (w), 1350 (w), 1243 (m), 1220 (m), 1205 (m), 1103 (m), 948 (w), 747 (s), 740 (w), 731 (w), 708 (w), 644 (m), 593 (w), 481 (w), 431 (w). Mp = 72−74 °C.

Preparation of $VCl(Py)_2(N^tBu)_2$ (6). To a solution of $VCl_2(NtBu)[NTMS(^tBu)]$ (675 mg, 2.0 mmol) in 25 mL of toluene was added pyridine (2.0 equiv, 161 μL, 2.0 mmol) via syringe. The reaction mixture was brought to reflux for 16 h. It was cooled and reduced to a residue in vacuo and extracted with toluene. The solution was transferred to a Schlenk tube via a filter cannula, and the filtrate was reduced until approximately 1 mL of red solution remained and copious amounts of solid were present. The solid was dissolved by warming the remaining solution to boiling. Cooling this solution to room temperature afforded the title compound in 33% (253 mg) yield as gold plates after decantation. X-ray-quality crystals were grown by the same method. ^1H NMR (C_6D_6, 600.1 MHz, 298 K) δ 9.08 (br s, *Ar*, 4H), 6.81 (br s, *Ar*, 2H), 6.53 (br s, *Ar*, 4H), 1.42 (s, N*t*Bu). $^{13}C\{^1H\}$ NMR (C_6D_6, 150.9 MHz, 298 K) δ 153.54 (s, *Ar*), 136.75 (s, *Ar*), 123.35 (s, *Ar*), 60.2* (α-N*t*Bu), 33.08 (s, β-*t*Bu). $^{51}V\{^1H\}$ NMR (C_6D_6, 157.8 MHz, 298 K) δ −485.42 (br s, $\Delta\nu_{1/2}$ = 20.19 Hz). Anal. Calcd for $C_{18}H_{28}N_4VCl$: C, 55.89; H, 7.30; N, 14.48. Found: C, 54.78; H, 7.03; N, 14.16 (carbon was consistently low on three attempts). IR (KBr, Nujol, cm^{-1}) 0.1603 (m), 1477 (w), 1438 (s), 1402 (w), 1356 (w), 1349 (w), 1333 (w), 1240 (m), 1215 (s), 1203 (s), 1151 (w), 1072 (w), 1063 (w), 1043 (w), 768 (w), 757 (w), 701 (s), 638 (w), 602 (w), 586 (m), 464 (w), 445 (w), 404 (w). Mp = 155 °C (decomp).

Preparation of $VBr(PMe_3)_2(N^tBu)_2$ (7). To a solution of $VCl(PMe_3)_2(N^tBu)_2$ (404 mg, 1.06 mmol) in 25 mL of toluene was added TMSBr (1.1 equiv, 140 μL, 1.17 mmol) via syringe. The reaction mixture was brought to reflux for 16 h. It was cooled and reduced to a residue in vacuo and extracted with hexane. The solution was transferred to a Schlenk tube via a filter cannula, and the filtrate was reduced until the product began to crystallize and was placed into a −40 °C freezer overnight. Recrystallization gave the title compound in 31% (140 mg) yield as dark green blocks after decantation. X-ray-quality crystals were grown by the same method. ^1H NMR ($CDCl_3$, 600.1 MHz, 298 K) δ 1.46 (unresolved t, PMe_3, 18H), 1.23 (s, *tBu*, 18H). $^{13}C\{^1H\}$ NMR ($CDCl_3$, 150.9 MHz, 298 K) δ 69.0* (α-*t*Bu), 33.56 (t, β-*t*Bu, $^4J_{CP}$ = 3.02 Hz), 17.16 (t, PMe_3, $^1J_{CP}$ = 10.86 Hz). $^{31}P\{^1H\}$ NMR ($CDCl_3$, 242.9 MHz, 298 K) δ −5.85 (br s, $\Delta\nu_{1/2}$ = 2223.42 Hz). $^{51}V\{^1H\}$ NMR ($CDCl_3$, 157.7 MHz, 298 K) δ −770.95 (br s, $\Delta\nu_{1/2}$ = 871.77 Hz). Anal. Calcd for $C_{14}H_{36}BrN_2P_2V$: C, 39.54; H, 8.53; N, 6.59. Found: C, 39.25; H, 8.53; N, 6.28. IR (KBr, Nujol, cm^{-1}): 1419 (m), 1350 (m), 1297 (m), 1279 (m), 1244 (s), 1221 (s), 1205 (s), 1106 (m), 951 (s), 846 (m), 734 (m), 594 (w). Mp = 110−112 °C.

Preparation of $VI(PMe_3)_2(N^tBu)_2$ (8). To a solution of $VCl(PMe_3)_2(N^tBu)_2$ (381 mg, 1.0 mmol) in 25 mL of toluene was added TMSI (1.0 equiv, 137 μL, 1.0 mmol) via syringe. The reaction mixture was brought to reflux for 16 h. It was cooled and reduced to a residue in vacuo and extracted with hexane. The solution was transferred to a Schlenk tube via a filter cannula, and the filtrate was reduced until the

dx.doi.org/10.1021/ic4020543 | *Inorg. Chem.* 2013, 52, 11650−11660

Table 5. Crystal and Refinement Data for Complexes 5, 6, 8, and 9

	5	6	8	9
empirical formula	$C_{24}H_{40}ClN_2P_2V$	$C_{18}H_{28}ClN_4V$	$C_{14}H_{36}IN_2P_2V$	$C_{20}H_{41}N_2P_2V$
formula weight	504.91	386.83	472.23	422.43
temp, K	100(2)	100(2)	100(2)	100(2)
λ	0.710 73	0.710 73	0.710 73	0.710 73
crystal system	monoclinic	orthorhombic	orthorhombic	monoclinic
space group	$P2_1/c$	*Pbca*	*Pbcm*	$P2_1/c$
a, Å	13.374(2)	9.504(2)	11.5148(13)	9.485(4)
b, Å	12.856(2)	18.182(4)	28.109(3)	9.550(4)
c, Å	16.237(3)	23.174(5)	14.1707(16)	27.830(11)
α, deg	90	90	90	90
β, deg	93.158(3)	90	90	95.873(7)
γ, deg	90	90	90	90
volume, Å^3	2787.4(9)	4004.7(15)	4586.7(9)	2507.6(17)
Z	4	8	8	4
d_{calc}, mg/m^3	1.203	1.283	1.368	1.119
F_{000}	1072	1632	1920	912
μ, mm^{-1}	0.579	0.635	1.914	0.529
no. of reflns measd	25126	134969	46440	22802
no. of indep reflns	5098	3692	4422	11343
R_{int}	0.0301	0.0636	0.0808	0.0676
restr/param	0/271	0/217	0/214	0/240
R_1, wR_2 [$I > 2\sigma(I)$]	0.0352, 0.0981	0.0325, 0.0765	0.0342, 0.0572	0.0958, 0.2211
R_1 (all data)	0.0504	0.0438	0.0627	0.1068
GOF	1.138	1.103	1.074	1.158
resid peak, hole (e$^-$/Å^3)	0.736, −0.561	0.486, −0.257	0.952, −0.641	0.617, −1.288

product began to crystallize and was placed into a −40 °C freezer overnight. Recrystallization afforded the title compound in 39% (185 mg) yield as colorless plates after decantation. X-ray-quality crystals were grown by the same method. ^{1}H NMR (CDCl3, 600.1 MHz, 298 K) δ 1.55 (unresolved t, PMe_3, 18H), 1.24 (s, *tBu*, 18H). $^{13}C\{^1H\}$ NMR ($CDCl_3$, 150.09 MHz, 298 K) δ 69.7* (α-*t*Bu), 33.32 (t, β-*t*Bu, $^4J_{CP}$ = 4.50 Hz) 18.35 (t, PMe_3, $^1J_{CP}$ = 11.24 Hz). $^{31}P\{^1H\}$ NMR ($CDCl_3$, 242.9 MHz, 298 K) δ −8.70 (br s, $\Delta\nu_{1/2}$ = 2179.95 Hz). $^{51}V\{^1H\}$ NMR ($CDCl_3$, 157.7 MHz, 298 K) δ −778.38 (br s, $\Delta\nu_{1/2}$ = 15.147 Hz). Anal. Calcd for $C_{14}H_{36}IN_2P_2V$: C, 35.61; H, 7.68; N, 5.93. Found: C, 35.54; H, 7.57; N, 5.79. IR (KBr, Nujol, cm^{-1}) 1420 (w), 1350 (w), 1296 (w), 1278 (m), 1242 (m), 1219 (s), 1203 (m), 1105 (m), 955 (s), 850 (w), 732 (m), 593 (m). Mp = 191−193 °C.

Preparation of $VPh(PMe_3)_2(N^tBu)_2$ (9). A solution of $VCl(PMe_3)_2(N^tBu)_2$ (400 mg, 1.05 mmol) in 25 mL of diethyl ether was added to a slurry of Ph_2Mg (1.2 equiv, 225 mg, 1.26 mmol) in 25 mL of diethyl ether at −78 °C via cannula. The reaction mixture was stirred for 1 h, allowed to warm to room temperature, and stirred for 4 h. The reaction mixture was then reduced to a residue in vacuo, extracted with hexane, and filtered via filter cannula. The filtrate was reduced in vacuo until the product began to crystallize. The saturated solution was then stored at −40 °C overnight to afford the product as bright yellow plates after decantation. A second crop was obtained by the same method to give 80 mg (18%) as combined yield. X-ray-quality crystals were grown by the same method. ^{1}H NMR (C_6D_6, 600.1 MHz, 298 K) δ 7.84 (m, *Ar*, 2H), 7.25 (t, *Ar*, 2H, J_{HH} = 7.20 Hz) 1.36 (s, *tBu*, 18H), 1.00 (pseudo d, P*Me*$_3$, J_{PH} = 7.20 Hz). $^{13}C\{^1H\}$ NMR (C_6D_6, 150.9 MHz, 298 K) δ 139.82 (t, *Ar*, J_{CP} = 5.28 Hz), 124.93 (t, *Ar*, J_{CP} = 4.83 Hz), 122.60 (t, *Ar*, J_{CP} = 4.38 Hz), 34.15 (t, β-*t*Bu, $^4J_{CP}$ = 3.02 Hz) 16.88 (dd, PMe_3, $^1J_{CP}$ = 11.92 Hz, $^3J_{CP}$ = 8.15 Hz). The α-*t*Bu resonance was not located. $^{31}P\{^1H\}$ NMR (C_6D_6, 161.96 MHz, 298 K) δ 1.07 (br s, $\Delta\nu_{1/2}$ = 1954.62 Hz). $^{51}V\{^1H\}$ NMR (C_6D_6, 105.2 MHz, 298 K) δ −801.07 (br s, $\Delta\nu_{1/2}$ = 21.87 Hz). Anal. Calcd for $C_{20}H_{41}N_2P_2V$: C, 56.86; H, 9.78; N, 6.63. Found: C, 56.48; H, 10.10; N, 6.36. IR (KBr, Nujol, cm^{-1}) 1347 (m), 1276 (m), 1247 (m), 1219 (s), 1203 (m), 1100 (m), 944 (s), 729 (s), 714 (m), 592 (m). Mp = 65 °C (decomp).

Vanadium L-Edge STXM Measurements. STXM methodology was similar to that discussed previously.[123,124] In an argon-filled glovebox, each sample was ground in a mortar and pestle, and the particles were transferred to a Si_3N_4 window (100 nm, Silson). A second window was placed over the sample, essentially sandwiching the particles, and the windows were sealed together with epoxy. V_2O_5 was dried at 150 °C and 0.01 mmHg for at least 24 h prior to V $L_{3,2}$-edge XANES measurements and handled with rigorous exclusion of air and moisture prior to and during use.

Single-energy images and vanadium L-edge XANES spectra were acquired on the STXM instrument at the Advanced Light Source−Molecular Environmental Science beamline 11.0.2, which is operated in topoff mode at 500 mA, in a ∼0.5 atm He-filled chamber.[125] An energy calibration was performed at the Ne K-edge for Ne (867.30 eV). For these measurements, the X-ray beam was focused with a zone plate onto the sample, and transmitted light was detected. The spot size and spectral resolution were determined from characteristics of the 35 nm zone plate. Images at a single energy were obtained by raster-scanning the sample and collecting transmitted monochromatic light as a function of sample position. Spectra at each image pixel or particular regions of interest on the sample image were extracted from the "stack", which is a collection of images recorded at multiple, closely spaced photon energies across the absorption edge.[126] Dwell times used to acquire an image at a single photon energy were ∼1 ms/pixel. To quantify the absorbance signal, the measured transmitted intensity (I) was converted to optical density via the Beer−Lambert law: OD = $\ln(I/I_0) = \mu\rho d$, where I_0 is the incident photon flux intensity, d is the sample thickness, and μ and ρ are the mass absorption coefficient and density of the sample material, respectively. Incident beam intensity was measured through the sample-free region of the Si_3N_4 windows. Regions of particles with an absorption of >1.5 OD were omitted to ensure the spectra were in the linear regime of the Beer−Lambert law. The energy resolution (full width at half-maximum, fwhm) was determined to be 0.08 eV, and spectra were collected by use of circularly polarized radiation. During the STXM experiment, particles showed no sign of radiation damage and each spectrum was reproduced from multiple independent particles. In typical data analysis, a first-order polynomial was fit to the pre-edge region (<514

dx.doi.org/10.1021/ic4020543 | *Inorg. Chem.* 2013, 52, 11650−11660

eV) and then subtracted from the experimental data to eliminate the background of the spectrum. Owing to the presence of adventitious oxygen and concomitant O K-edge absorptions above 530 eV, the V $L_{3,2}$-edge absorptions could not be rigorously normalized.

General Remarks on Determination of Molecular Structure by X-ray Diffraction. X-ray diffraction data were collected on either Bruker AXS three-circle or Bruker AXS Microstar κ-geometry diffractometers with either graphite-monochromated Mo Kα radiation (λ = 0.710 73 Å) or Helios-monochromated Cu Kα radiation (λ = 1.541 78 Å). A single crystal of appropriate size was coated in Paratone-N oil and mounted on a cryo loop. The loop was transferred to a diffractometer equipped with a charge-coupled device (CCD) area detector,[103] centered in the beam, and cooled by an Oxford Cryostream 700 LT device. Preliminary orientation matrices and cell constants were determined by collection of three sets of 40 5-s frames or three sets of 30 10-s frames, followed by spot integration and least-squares refinement. COSMO was used to determine an appropriate data collection strategy, and the raw data were integrated by use of SAINT.[104] Cell dimensions reported were calculated from all reflections with $I > 10\sigma$. The data were corrected for Lorentz and polarization effects; no correction for crystal decay was applied. Data were analyzed for agreement and possible absorption by use of XPREP.[105] An absorption correction based on comparison of redundant and equivalent reflections was applied by use of SADABS.[106] Structures were solved by direct methods with the aid of successive difference Fourier maps and were refined on F^2 by use of the SHELXTL 5.0 software package. All non-hydrogen atoms were refined anisotropically; all hydrogen atoms were included into the model at their calculated positions and refined using a riding model. For all structures, $R_1 = \sum(|F_o| - |F_c|)/\sum(|F_o|)$ and $wR_2 = \{\sum[w(F_o^2 - F_c^2)^2]/\sum[w(F_o^2)^2]\}^{1/2}$. See Table 5 for details.

■ ASSOCIATED CONTENT

Supporting Information

Crystallographic information (CIF). This material is available free of charge via the Internet at http://pubs.acs.org.

■ AUTHOR INFORMATION

Corresponding Authors

*(J.A.) E-mail arnold@berkeley.edu.
*(R.G.B.) E-mail rbergman@berkeley.edu
*(F.D.T.) E-mail fdtoste@berkeley.edu

Present Address

‖(H.S.LaP.) Department of Chemistry and Pharmacy, Inorganic Chemistry, University of Erlangen−Nürnberg, 91058 Erlangen, Germany.

Notes

The authors declare no competing financial interest.

■ ACKNOWLEDGMENTS

H.S.LaP. acknowledges the support of NSF for a predoctoral fellowship and the UCB Department of Chemistry for the Dauben Fellowship. We thank Dr. Christopher Canlas for experimental assistance, and Professor Richard A. Andersen, Dr. Gregory Nocton, Dr. Neil C. Tomson, and Thomas L. Gianetti for helpful discussions. This work was supported at UC—Berkeley by the AFOSR (11RSA093). The MES Beamline 11.0.2 was supported by the Director, Office of Science, Office of Basic Energy Sciences, Division of Chemical Sciences, Geosciences, and Biosciences (CSGB) and the CSGB Condensed Phase and Interfacial Molecular Sciences program, both of the U.S. Department of Energy at Lawrence Berkeley National Laboratory under Contract No. DE-AC02-05CH11231. T.T. and the ALS were supported by Director, Office of Science, Office of Basic Energy Sciences of the U.S. Department of Energy at LBNL under Contract No. DE-AC02-05CH11231. D.K.S and S.G.M. (in part) were supported by Director, Office of Science, Office of Basic Energy Sciences and by the Division of Chemical Sciences, Geosciences, and Biosciences, Heavy Element Chemistry program of the U.S. Department of Energy at LBNL under Contract DE-AC02-05CH11231. S.A.K. was supported under the Heavy Element Chemistry Program at LANL by the Division of Chemical Sciences, Geosciences, and Biosciences, Office of Basic Energy Sciences, U.S. Department of Energy. Los Alamos National Laboratory is operated by Los Alamos National Security, LLC, for the National Nuclear Security Administration of U.S. Department of Energy under Contract DE-AC52-06NA25396. Parts of this work were also supported at LANL by the Glenn T. Seaborg Institute postdoctoral fellowships (S.G.M.).

■ REFERENCES

(1) Schwarz, A. D.; Nova, A.; Clot, E.; Mountford, P. *Chem. Commun.* **2011**, *47*, 4926.
(2) Schwarz, A. D.; Nova, A.; Clot, E.; Mountford, P. *Inorg. Chem.* **2011**, *50*, 12155.
(3) Schofield, A. D.; Nova, A.; Selby, J. D.; Manley, C. D.; Schwarz, A. D.; Clot, E.; Mountford, P. *J. Am. Chem. Soc.* **2010**, *132*, 10484.
(4) Bolton, P. D.; Feliz, M.; Cowley, A. R.; Clot, E.; Mountford, P. *Organometallics* **2008**, *27*, 6096.
(5) Ignatov, S. K.; Rees, N. H.; Merkoulov, A. A.; Dubberley, S. R.; Razuvaev, A. G.; Mountford, P.; Nikonov, G. I. *Organometallics* **2008**, *27*, 5968.
(6) Cloke, F. G. N.; Green, J. C.; Hazari, N.; Hitchcock, P. B.; Mountford, P.; Nixon, J. F.; Wilson, D. J. *Organometallics* **2006**, *25*, 3688.
(7) Gerber, L. C. H.; Schrock, R. R.; Muller, P.; Takase, M. K. *J. Am. Chem. Soc.* **2011**, *133*, 18142.
(8) Meek, S. J.; O'Brien, R. V.; Llaveria, J.; Schrock, R. R.; Hoveyda, A. H. *Nature* **2011**, *471*, 461.
(9) Gianetti, T. L.; Tomson, N. C.; Arnold, J.; Bergman, R. G. *J. Am. Chem. Soc.* **2011**, *133*, 14904.
(10) Tomson, N. C.; Arnold, J.; Bergman, R. G. *Dalton Trans.* **2011**, *40*, 7718.
(11) Tomson, N. C.; Arnold, J.; Bergman, R. G. *Organometallics* **2010**, *29*, 5010.
(12) Tomson, N. C.; Arnold, J.; Bergman, R. G. *Organometallics* **2010**, *29*, 2926.
(13) Tomson, N. C.; Yan, A.; Arnold, J.; Bergman, R. G. *J. Am. Chem. Soc.* **2008**, *130*, 11262.
(14) Khalimon, A. Y.; Ignatov, S. K.; Simionescu, R.; Kuzmina, L. G.; Howard, J. A. K.; Nikonov, G. I. *Inorg. Chem.* **2012**, *51*, 754.
(15) Khalimon, A. Y.; Farha, P.; Kuzmina, L. G.; Nikonov, G. I. *Chem. Commun.* **2012**, *48*, 455.
(16) Nikonov, G. I.; Khalimon, A. Y.; Simionescu, R. *J. Am. Chem. Soc.* **2011**, *133*, 7033.
(17) Mountford, P.; Ignatov, S. K.; Khalimon, A. Y.; Rees, N. H.; Razuvaev, A. G.; Nikonov, G. I. *Inorg. Chem.* **2009**, *48*, 9605.
(18) Khalimon, A. Y.; Simionescu, R.; Kuzmina, L. G.; Howard, J. A. K.; Nikonov, G. I. *Angew. Chem., Int. Ed.* **2008**, *47*, 7701.
(19) Khalimon, A. Y.; Holland, J. P.; Kowalczyk, R. M.; McInnes, E. J. L.; Green, J. C.; Mountford, P.; Nikonov, G. I. *Inorg. Chem.* **2008**, *47*, 999.
(20) Schwarz, A. D.; Nielson, A. J.; Kaltsoyannis, N.; Mountford, P. *Chem. Sci.* **2012**, *3*, 819.
(21) La Pierre, H. S.; Arnold, J.; Toste, F. D. *Angew. Chem., Int. Ed.* **2011**, *50*, 3900.
(22) La Pierre, H. S.; Arnold, J.; Bergman, R. G.; Toste, F. D. *Inorg. Chem.* **2012**, *51*, 13334.
(23) Gianetti, T. L.; La Pierre, H. S.; Arnold, J. *Eur. J. Inorg. Chem.* **2013**, No. 22−23, 3771.
(24) Nugent, W. A.; Haymore, B. L. *Coord. Chem. Rev.* **1980**, *31*, 123.

(25) Nugent, W. A.; Mayer, J. M. *Metal-Ligand Multiple Bonds*; Wiley: New York, 1988.
(26) Wigley, D. E. *Prog. Inorg. Chem.* **1994**, 239.
(27) Williams, D. S.; Schofield, M. H.; Schrock, R. R. *Organometallics* **1993**, *12*, 4560.
(28) Albright, T. A.; Burdett, J. K.; Whangbo, M. H. *Orbital Interactions in Chemistry*; John Wiley & Sons: New York, 1985.
(29) Lauher, J. W.; Hoffmann, R. *J. Am. Chem. Soc.* **1976**, *98*, 1729.
(30) Brintzinger, H. H.; Lohr, L. L.; Wong, K. L. T. *J. Am. Chem. Soc.* **1975**, *97*, 5146.
(31) Ciszewski, J. T.; Harrison, J. F.; Odom, A. L. *Inorg. Chem.* **2004**, *43*, 3605.
(32) Nugent, W. A.; Harlow, R. L. *Inorg. Chem.* **1980**, *19*, 777.
(33) Meijboom, N.; Schaverien, C. J.; Orpen, A. G. *Organometallics* **1990**, *9*, 774.
(34) Leung, W. H.; Danopoulos, A. A.; Wilkinson, G.; Hussainbates, B.; Hursthouse, M. B. *J. Chem. Soc., Dalton Trans.* **1991**, 2051.
(35) Nugent, W. A.; Harlow, R. L. *J. Am. Chem. Soc.* **1980**, *102*, 1759.
(36) Lam, H. W.; Wilkinson, G.; Hussainbates, B.; Hursthouse, M. B. *J. Chem. Soc., Dalton Trans.* **1993**, 1477.
(37) Hursthouse, M. B.; Motevalli, M.; Sullivan, A. C.; Wilkinson, G. *J. Chem. Soc. Chem. Commun.* **1986**, 1398.
(38) Sullivan, A. C.; Wilkinson, G.; Motevalli, M.; Hursthouse, M. B. *J. Chem. Soc., Dalton Trans.* **1988**, 53.
(39) Danopoulos, A. A.; Leung, W. H.; Wilkinson, G.; Hussainbates, B.; Hursthouse, M. B. *Polyhedron* **1990**, *9*, 2625.
(40) Danopoulos, A. A.; Wilkinson, G. *Polyhedron* **1990**, *9*, 1009.
(41) Chan, D. M. T.; Nugent, W. A. *Inorg. Chem.* **1985**, *24*, 1422.
(42) Chan, D. M. T.; Fultz, W. C.; Nugent, W. A.; Roe, D. C.; Tulip, T. H. *J. Am. Chem. Soc.* **1985**, *107*, 251.
(43) Williams, D. S.; Anhaus, J. T.; Schofield, M. H.; Schrock, R. R.; Davis, W. M. *J. Am. Chem. Soc.* **1991**, *113*, 5480.
(44) Williams, D. S.; Schofield, M. H.; Anhaus, J. T.; Schrock, R. R. *J. Am. Chem. Soc.* **1990**, *112*, 6728.
(45) Williams, D. S.; Schrock, R. R. *Organometallics* **1993**, *12*, 1148.
(46) Schofield, M. H.; Kee, T. P.; Anhaus, J. T.; Schrock, R. R.; Johnson, K. H.; Davis, W. M. *Inorg. Chem.* **1991**, *30*, 3595.
(47) Chong, A. O.; Oshima, K.; Sharpless, K. B. *J. Am. Chem. Soc.* **1977**, *99*, 3420.
(48) Schaller, C. P.; Wolczanski, P. T. *Inorg. Chem.* **1993**, *32*, 131.
(49) Dewith, J.; Horton, A. D. *Angew. Chem., Int. Ed.* **1993**, *32*, 903.
(50) Kennedy-Smith, J. J.; Nolin, K. A.; Gunterman, H. P.; Toste, F. D. *J. Am. Chem. Soc.* **2003**, *125*, 4056.
(51) Nolin, K. A.; Ahn, R. W.; Toste, F. D. *J. Am. Chem. Soc.* **2005**, *127*, 12462.
(52) Nolin, K. A.; Krumper, J. R.; Pluth, M. D.; Bergman, R. G.; Toste, F. D. *J. Am. Chem. Soc.* **2007**, *129*, 14684.
(53) Toste, F. D.; Nolin, K. A.; Ahn, R. W.; Kobayashi, Y.; Kennedy-Smith, J. J. *Chem.—Eur. J.* **2010**, *16*, 9555.
(54) Walsh, P. J.; Hollander, F. J.; Bergman, R. G. *J. Am. Chem. Soc.* **1988**, *110*, 8729.
(55) Sweeney, Z. K.; Salsman, J. L.; Andersen, R. A.; Bergman, R. G. *Angew. Chem., Int. Ed.* **2000**, *39*, 2339.
(56) Sweeney, Z. K.; Polse, J. L.; Bergman, R. G.; Andersen, R. A. *Organometallics* **1999**, *18*, 5502.
(57) Polse, J. L.; Andersen, R. A.; Bergman, R. G. *J. Am. Chem. Soc.* **1998**, *120*, 13405.
(58) Parkin, G.; Bercaw, J. E. *J. Am. Chem. Soc.* **1989**, *111*, 391.
(59) Blake, R. E.; Antonelli, D. M.; Henling, L. M.; Schaefer, W. P.; Hardcastle, K. I.; Bercaw, J. E. *Organometallics* **1998**, *17*, 718.
(60) Cummins, C. C.; Baxter, S. M.; Wolczanski, P. T. *J. Am. Chem. Soc.* **1988**, *110*, 8731.
(61) Cummins, C. C.; Schaller, C. P.; Vanduyne, G. D.; Wolczanski, P. T.; Chan, A. W. E.; Hoffmann, R. *J. Am. Chem. Soc.* **1991**, *113*, 2985.
(62) Schafer, D. F.; Wolczanski, P. T. *J. Am. Chem. Soc.* **1998**, *120*, 4881.
(63) Ignatov, S. K.; Rees, N. H.; Dubberley, S. R.; Razuvaev, A. G.; Mountford, P.; Nikonov, G. I. *Chem. Commun.* **2004**, 952.
(64) Mountford, P.; Ignatov, S. K.; Rees, N. H.; Merkoulov, A. A.; Dubberley, S. R.; Razuvaev, A. G.; Nikonov, G. I. *Chem.—Eur. J.* **2008**, *14*, 296.
(65) Milsmann, C.; Turner, Z. R.; Semproni, S. P.; Chirik, P. J. *Angew. Chem., Int. Ed.* **2012**, *51*, 5386.
(66) Dewith, J.; Horton, A. D.; Orpen, A. G. *Organometallics* **1990**, *9*, 2207.
(67) Dewith, J.; Horton, A. D.; Orpen, A. G. *Organometallics* **1993**, *12*, 1493.
(68) Preuss, F.; Becker, H.; Wieland, T. *Z. Naturforsch., B: J. Chem. Sci.* **1990**, 191.
(69) Kilgore, U. J.; Karty, J. A.; Pink, M.; Gao, X.; Mindiola, D. J. *Angew. Chem., Int. Ed.* **2009**, *48*, 2394.
(70) Tsai, Y.; Wang, P.; Lin, K.; Chen, S.; Chen, J. *Chem. Commun.* **2008**, 205.
(71) Chao, Y. W.; Wexler, P. A.; Wigley, D. E. *Inorg. Chem.* **1990**, *29*, 4592.
(72) Preuss, F.; Towae, W. *Z. Naturforsch., B: Anorg. Chem., Org. Chem.* **1981**, *36*, 1130.
(73) Walter, M. D.; White, P. S. *Inorg. Chem.* **2012**, *51*, 11860.
(74) Devore, D. D.; Lichtenhan, J. D.; Takusagawa, F.; Maatta, E. A. *J. Am. Chem. Soc.* **1987**, *109*, 7408.
(75) Landis, C. R.; Uddin, J.; Morales, C. M.; Maynard, J. H. *Organometallics* **2006**, *25*, 5566.
(76) Hawkeswood, S. B.; Stephan, D. W. *Inorg. Chem.* **2003**, *42*, 5429.
(77) Tolman, C. A. *Chem. Rev.* **1977**, *77*, 313.
(78) Immirzi, A.; Musco, A. *Inorg. Chim. Acta* **1977**, *25*, L41.
(79) Nugent, W. A.; Mckinney, R. J.; Kasowski, R. V.; Vancatledge, F. A. *Inorg. Chim. Acta* **1982**, *65*, L91.
(80) Rehder, D. *Coord. Chem. Rev.* **2008**, *252*, 2209.
(81) Minasian, S. G.; Keith, J. M.; Batista, E. R.; Boland, K. S.; Kozimor, S. A.; Martin, R. L.; Shuh, D. K.; Tyliszczak, T.; Vernon, L. J. *J. Am. Chem. Soc.* 2013, in press; DOI: 10.1021/ja405844j.
(82) Kozimor, S. A.; Yang, P.; Batista, E. R.; Boland, K. S.; Burns, C. J.; Clark, D. L.; Conradson, S. D.; Martin, R. L.; Wilkerson, M. P.; Wolfsberg, L. E. *J. Am. Chem. Soc.* **2009**, *131*, 12125.
(83) Kozimor, S. A.; Yang, P.; Batista, E. R.; Boland, K. S.; Burns, C. J.; Christensen, C. N.; Clark, D. L.; Conradson, S. D.; Hay, P. J.; Lezama, J. S.; Martin, R. L.; Schwarz, D. E.; Wilkerson, M. P.; Wolfsberg, L. E. *Inorg. Chem.* **2008**, *47*, 5365.
(84) George, S. D.; Brant, P.; Solomon, E. I. *J. Am. Chem. Soc.* **2005**, *127*, 667.
(85) Casarin, M.; Finetti, P.; Vittadini, A.; Wang, F.; Ziegler, T. *J. Phys. Chem. A* **2007**, *111*, 5270.
(86) Wen, A. T.; Hitchcock, A. P. *Can. J. Chem.* **1993**, *71*, 1632.
(87) Spencer, L. P.; Yang, P.; Minasian, S. G.; Jilek, R. E.; Batista, E. R.; Boland, K. S.; Boncella, J. M.; Conradson, S. D.; Clark, D. L.; Hayton, T. W.; Kozimor, S. A.; Martin, R. L.; MacInnes, M. M.; Olson, A. C.; Scott, B. L.; Shuh, D. K.; Wilkerson, M. P. *J. Am. Chem. Soc.* **2013**, *135*, 2279.
(88) Sawatzky, G. A.; Post, D. *Phys. Rev. B* **1979**, *20*, 1546.
(89) Collison, D.; Gahan, B.; Garner, C. D.; Mabbs, F. E. *J. Chem. Soc., Dalton Trans.* **1980**, 667.
(90) Abbate, M.; Degroot, F. M. F.; Fuggle, J. C.; Ma, Y. J.; Chen, C. T.; Sette, F.; Fujimori, A.; Ueda, Y.; Kosuge, K. *Phys. Rev. B* **1991**, *43*, 7263.
(91) Brackemeyer, T.; Erker, G.; Frohlich, R. *Organometallics* **1997**, *16*, 531.
(92) Havecker, M.; Knop-Gericke, A.; Mayer, R. W.; Fait, M.; Bluhm, H.; Schlogl, R. *J. Electron Spectrosc. Relat. Phenom.* **2002**, *125*, 79.
(93) Zhang, G. P.; Callcott, T. A.; Woods, G. T.; Lini, L.; Sales, B.; Mandrus, D.; He, J. *Phys. Rev. Lett.* **2002**, *88*, No. 077401.
(94) Zhang, G. P.; Woods, G. T.; Shirley, E. L.; Callcott, T. A.; Lin, L.; Chang, G. S.; Sales, B. C.; Mandrus, D.; He, J. *Phys. Rev. B* **2002**, *65*, No. 165107.
(95) Fagin, A. A.; Bochkarev, M. N.; Kozimor, S. A.; Ziller, J. W.; Evans, W. J. *Z. Anorg. Allg. Chem.* **2005**, *631*, 2848.

(96) Abadie, J.; Abbott, B. P.; Abbott, R.; Accadia, T.; Acernese, F.; Adhikari, R.; Ajith, P.; Allen, B.; Allen, G.; Ceron, E. A.; Amin, R. S.; Anderson, S. B.; Anderson, W. G.; Antonucci, F.; Arain, M. A.; Araya, M.; Arun, K. G.; Aso, Y.; Aston, S.; Astone, P.; Aufmuth, P.; Aulbert, C.; Babak, S.; Baker, P.; Ballardin, G.; Ballmer, S.; Barker, D.; Barone, F.; Barr, B.; Barriga, P.; Barsotti, L.; Barsuglia, M.; Barton, M. A.; Bartos, I.; Bassiri, R.; Bastarrika, M.; Bauer, T. S.; Behnke, B.; Beker, M. G.; Belletoile, A.; Benacquista, M.; Betzwieser, J.; Beyersdorf, P. T.; Bigotta, S.; Bilenko, I. A.; Billingsley, G.; Birindelli, S.; Biswas, R.; Bizouard, M. A.; Black, E.; Blackburn, J. K.; Blackburn, L.; Blair, D.; Bland, B.; Blom, M.; Boccara, C.; Bock, O.; Bodiya, T. P.; Bondarescu, R.; Bondu, F.; Bonelli, L.; Bonnand, R.; Bork, R.; Born, M.; Bose, S.; Bosi, L.; Bouhou, B.; Braccini, S.; Bradaschia, C.; Brady, P. R.; Braginsky, V. B.; Brau, J. E.; Breyer, J.; Bridges, D. O.; Brillet, A.; Brinkmann, M.; Brisson, V.; Britzger, M.; Brooks, A. F.; Brown, D. A.; Budzynski, R.; Bulik, T.; Bullington, A.; Bulten, H. J.; Buonanno, A.; Burmeister, O.; Buskulic, D.; Buy, C.; Byer, R. L.; Cadonati, L.; Cagnoli, G.; Cain, J.; Calloni, E.; Camp, J. B.; Campagna, E.; Cannizzo, J.; Cannon, K. C.; Canuel, B.; Cao, J.; Capano, C. D. *Astrophys. J.* **2010**, *81*, 1453.
(97) Hellmann, I.; Taeschner, C.; Klingeler, R.; Leonhardt, A.; Buechner, B.; Knupfer, M. *J. Chem. Phys.* **2008**, *128*, 224701−1.
(98) Fronzoni, G.; Stener, M.; Decleva, P.; de Simone, M.; Coreno, M.; Franceschi, P.; Furlani, C.; Prince, K. C. *J. Phys. Chem. A* **2009**, *113*, 2914.
(99) Abbate, M.; Pen, H.; Czyzyk, M. T.; Degroot, F. M. F.; Fuggle, J. C.; Ma, Y. J.; Chen, C. T.; Sette, F.; Fujimori, A.; Ueda, Y.; Kosuge, K. *J. Electron Spectrosc. Relat. Phenom.* **1993**, *62*, 185.
(100) Chen, J. G.; Kim, C. M.; Fruhberger, B.; Devries, B. D.; Touvelle, M. S. *Surf. Sci.* **1994**, *321*, 145.
(101) Goering, E.; Muller, O.; Klemm, M.; denBoer, M. L.; Horn, S. *Philos. Mag. B* **1997**, *75*, 229.
(102) Su, D. S.; Zandbergen, H. W.; Tiemeijer, P. C.; Kothleitner, G.; Havecker, M.; Hebert, C.; Knop-Gericke, A.; Freitag, B. H.; Hofer, F.; Schlogl, R. *Micron* **2003**, *34*, 235.
(103) Woll, C.; Khyzhun, O. Y.; Strunskus, T.; Grunert, W. *J. Electron Spectrosc. Relat. Phenom.* **2005**, *149*, 20979.
(104) Brik, M. G.; Ogasawara, K.; Ikeno, H.; Tanaka, I. *Eur. Phys. J. B* **2006**, *51*, 345.
(105) De Francesco, R.; Stener, M.; Causa, M.; Toffoli, D.; Fronzoni, G. *Phys. Chem. Chem. Phys.* **2006**, *8*, 4300.
(106) Ma, C.; Yang, H. X.; Li, Z. A.; Ueda, Y.; Li, J. Q. *Solid State Commun.* **2008**, *146*, 30.
(107) Patridge, C. J.; Jaye, C.; Abtew, T. A.; Ravel, B.; Fischer, D. A.; Marschilok, A. C.; Zhang, P.; Takeuchi, K. J.; Takeuchi, E. S.; Banerjee, S. *J. Phys. Chem. C* **2011**, *115*, 14437.
(108) Grigg, J.; Collison, D.; Garner, C. D.; Helliwell, M.; Tasker, P. A.; Thorpe, J. M. *J. Chem. Soc., Chem. Commun.* **1993**, 1807.
(109) Collison, D.; Garner, C. D.; Grigg, J.; McGrath, C. M.; Mosselmans, J. F. W.; Pidcock, E.; Roper, M. D.; Seddon, J. M. W.; Sinn, E.; Tasker, P. A.; Thornton, G.; Walsh, J. F.; Young, N. A. *J. Chem. Soc., Dalton Trans.* **1998**, 2199.
(110) Solomon, E. I.; Lever, A. B. P. *Inorganic Electronic Structure and Spectroscopy*; John Wiley & Sons: Hoboken, NJ, 2006; Vol. 2.
(111) de Groot, F. *Coord. Chem. Rev.* **2005**, *249*, 31.
(112) Vanderlaan, G.; Kirkman, I. W. *Condens. Matter* **1992**, *4*, 4189.
(113) Goering, E.; Muller, O.; Klemm, M.; denBoer, M. L.; Horn, S. *Philos. Mag. B* **1997**, *75*, 229.
(114) Degroot, F. M. F. *J. Electron Spectrosc. Relat. Phenom.* **1994**, *67*, 529.
(115) Solomon, E. I.; Hedman, B.; Hodgson, K. O.; Dey, A.; Szilagyi, R. K. *Coord. Chem. Rev.* **2005**, *249*, 97.
(116) Rehder, D.; Polenova, T.; Buhl, M. *Annu. Rep. NMR Spectrosc.* **2007**, *62*, 49.
(117) Cummins, C. C.; Schrock, R. R.; Davis, W. M. *Inorg. Chem.* **1994**, *33*, 1448.
(118) Gerlach, C. P.; Arnold, J. *Inorg. Chem.* **1996**, *35*, 5770.
(119) Luetkens, M. L.; Sattelberger, A. P.; Murray, H. H.; Basil, J. D.; Fackler, J. P.; Jones, R. A.; Heaton, D. E. *Inorg. Synth.* **1990**, *28*, 305.
(120) Krossing, I. *Chem.—Eur. J.* **2001**, *7*, 490.
(121) Andersen, R. A.; Wilkinson, G. *J. Chem. Soc., Dalton Trans.* **1977**, 809.
(122) Preuss, F.; Fuchslocher, E.; Leber, E.; Towae, W. *Z. Naturforsch., B: J. Chem. Sci.* **1989**, *44*, 271.
(123) Bradley, J. A.; Yang, P.; Batista, E. R.; Boland, K. S.; Burns, C. J.; Clark, D. L.; Conradson, S. D.; Kozimor, S. A.; Martin, R. L.; Seidler, G. T.; Scott, B. L.; Shuh, D. K.; Tyliszczak, T.; Wilkerson, M. P.; Wolfsberg, L. E. *J. Am. Chem. Soc.* **2010**, *132*, 13914.
(124) Minasian, S. G.; Keith, J. M.; Batista, E. R.; Boland, K. S.; Bradley, J. A.; Daly, S. R.; Sokaras, D.; Kozimor, S. A.; Lukens, W. W.; Martin, R. L.; Nordlund, D.; Seidler, G. T.; Shuh, D. K.; Tyliszczak, T.; Wagner, G. L.; Wang, T. C.; Yang, P. *J. Am. Chem. Soc.* **2013**, *135*, 1864.
(125) Bluhm, H.; K. A.; Araki, T.; Benzerara, K.; Brown, G. E.; Dynes, J. J.; Ghosal, S.; Gilles, M. K.; Hansen, H. C.; Hemminger, J. C.; Hitchcock, A. P.; Ketteler, G.; Kilcoyne, A. L. D.; Kneedler, E.; Lawrence, J. R.; Leppard, G. G.; Majzlan, J.; Mun, B. S.; Myneni, S. C. B.; Nilsson, A.; Ogasawara, H.; Ogletree, D. F.; Pecher, K.; Salmeron, M.; Shuh, D. K.; Tonner, B.; Tyliszczak, T.; Warwick, T.; Yoon, T. H. *J. Electron Spectrosc. Relat. Phenom.* **2006**, *150*, 86.
(126) Hitchcock, A. P. *aXis, version 17*; McMaster University, Hamilton, Ontario, Canada, 2008.